Available online at www.sciencedirect.com
ScienceDirect
Journal of Power Sources 160 (2006) 789–795
JOURNAL OF POWER SOURCES
www.elsevier.com/locate/jpowsour

Solubility and electrochemical studies of $LiFeO_2$–$LiCoO_2$–NiO materials for the MCFC cathode application

Armelle Ringuedé [a,*], Athula Wijayasinghe [b,d], Valérie Albin [a], Carina Lagergren [c], Michel Cassir [a], Bill Bergman [b]

[a] *Laboratoire d'Electrochimie et de Chimie Analytique, UMR 7575 CNRS-ENSCP, 11 rue Pierre et Marie Curie, 75231 Paris Cedex 05, France*
[b] *Department of Materials Science and Engineering, KTH, Royal Institute of Technology, Sweden*
[c] *Department of Chemical Engineering and Technology, KTH, Royal Institute of Technology, Sweden*
[d] *Institute of Fundamental Studies, Kandy, Sri Lanka*
Available online 12 June 2006

Abstract

The dissolution of the state-of-the-art lithiated NiO is still considered as one of the main obstacles to the commercialisation of the molten carbonate fuel cell (MCFC). Development of alternative cathode materials has been considered as a main strategy for solving this problem. Ternary compositions of $LiFeO_2$, $LiCoO_2$ and NiO are expected to decrease the cathode solubility while ensuring a good electrical conductivity and electrochemical activity towards the oxygen reduction.

In this work, new material compositions in the $LiFeO_2$–$LiCoO_2$–NiO ternary system were synthesised using Pechini method and investigating their electrical conductivity by the DC four probe method. Then the influence of the cobalt content in the composition was determined in terms of AC impedance analysis and solubility measurements after 200 h of immersion in Li_2CO_3–Na_2CO_3 at 650 °C. The DC electrical conductivity study reveals the ability of improving the electrical conductivity, adequate for MCFC cathode application, by controlling the Co content of the composition. A special attention was given to the evolution of the open circuit potential as a function of time and to the impedance spectroscopy characterization related to microstructure modifications. Taking into account solubility, electrical conductivity, as well as electrochemical performance in the fuel cell, this study reveals the possibility of using $LiFeO_2$–$LiCoO_2$–NiO ternary materials for MCFC cathode.

Keywords: MCFC; Cathode; $LiFeO_2$–$LiCoO_2$–NiO ternary materials; Open circuit potential; Solubility; Impedance spectroscopy

1. Introduction

The dissolution of the state-of-the-art lithiated NiO cathode material is considered as a major lifetime limiting factor and a major obstacle for the development of the molten carbonate fuel cell (MCFC) technology [1,2]. Modification of the electrolyte composition, by increasing its basicity, is considered as a solution to overcome this obstacle [3–5]; however, it may lead to a performance decrease. Another solution is the modification of the state-of-the-art NiO cathode material. Some authors have proposed the protection of this Ni-based cathode by a cobalt-based oxide layer [6,7]. On the other hand, development of alternative cathode materials is considered as a main strategy to solve the cathode dissolution problem.

In searching for new cathode materials, the emphasis should be mainly given to the stability of the candidate materials under MCFC working conditions. Moreover, the candidate material should possess an adequate electrical conductivity and electrocatalytic activity [8]. $LiFeO_2$ and $LiCoO_2$, which were earlier supposed to be the most promising candidates, have been extensively studied; however, none of them could directly substitute lithiated NiO. Though $LiFeO_2$ shows a negligible dissolution rate, the cathodes showed very low performance due to intrinsic materials' properties, such as poor oxygen reduction kinetics and electrical conductivity. On the other hand, porous $LiCoO_2$ cathodes show sufficient electrical conductivity but their low mechanical strength and high cost have limited their practical use in MCFC stacks. Moreover, considerably high contact resistance of $LiCoO_2$ cathodes with the current collector have obstructed the direct substitution of lithiated NiO by $LiCoO_2$ for [9–11].

The possibility of improving these single candidates, doping or forming into mixed oxides, has also been investigated.

* Corresponding author. Tel.: +33 1 55 42 12 35; fax: +33 1 44 27 67 50.
E-mail addresses: armelle-ringuede@enscp.fr (A. Ringuedé), michel-cassir@enscp.fr (M. Cassir).

0378-7753/$ – see front matter © 2006 Elsevier B.V. All rights reserved.
doi:10.1016/j.jpowsour.2006.04.136

Makkus et al. [12] reported similar electrochemical behavior but different performances due to differences in electrical conductivity, specific surface area, chemical stability, etc. for lithiated NiO, Co-doped $LiFeO_2$ and $LiCoO_2$ cathodes. Therefore, it was suggested that a mixture of these oxides should combine the desirable properties of each single candidate, hence, forming a better material. Based on their work performed on selected $LiFeO_2$–$LiCoO_2$–NiO compositions, Bloom et al. [13] proposed these materials because of their low resistivity with adequate electrocatalytic activity. Moreover, Kudo et al. [14] showed, for Ni–Fe–Co ternary oxides, that the Ni^{2+} solubility decreases with the increase in the Fe content. Hence, these $LiFeO_2$–$LiCoO_2$–NiO materials can be suggested more viable alternatives to lithiated NiO.

Our studies on $LiFeO_2$–$LiCoO_2$–NiO compositions have revealed promising electrical conductivity and cell performance of these materials for MCFC cathode application [15–17]. Together with a summary of the synthesis and material characterization of these ternary compositions, this paper presents solubility and electrochemical characterization studies performed on some selected $LiFeO_2$–$LiCoO_2$–NiO materials prepared in this study.

2. Experimental

2.1. Material preparation

The Pechini method [18] was used for powder preparation with the metal nitrates, $LiNO_3$, $Fe(NO_3)_3{\cdot}9H_2O$, $Ni(NO_3)_2{\cdot}6H_2O$ and $Co(NO_3)_2{\cdot}6H_2O$ (Merck, Germany) of analysis grade as the starting materials. Stoichiometric amounts of the metal nitrates were thoroughly mixed with citric acid and ethylene glycol (Merck, Germany) using a magnetic stirrer hot plate, at room temperature for about 20 h. Thereafter the temperature was raised to 60 °C to obtain a viscous resin, which was on further heating subsequently charred to ash at 350 °C, and then calcined at 650 °C for 2 h in air. The calcined powder was pressed at 100 MPa and the green pellets (12 mm in diameter) were subsequently sintered at 1000 °C for 2 h in air.

2.2. Material characterization

X-ray diffraction (XRD, Philips diffractometer using monochromatic Cu Kα radiation) was used for phase analysis of the sintered materials. DC electrical conductivity measurements were performed on sintered pellets by the four probe method. Before the measurements, the flat end surfaces of pellets were coated with gold paste (G3535, Agar Scientific Ltd., England) or platinum paste (6402 0040/308A, Germany). The electrical conductivity measurements were performed in air and cathode gas (30% CO_2 + 70% air), in the temperature range between 550 and 750 °C.

2.3. Electrochemical characterizations

Electrochemical characterization consisted in chronopotentiometric measurements, without DC current, and impedance spectroscopy. The studied material was considered as the working electrode. Gold wire was used as the counter-electrode and the reference electrode was the Ag^+/Ag system, constituted by a silver wire immersed in the molten electrolyte mixture, saturated by Ag_2SO_4. The electrolyte was a mixture of Li_2CO_3–Na_2CO_3 (52–48 mole%), molten at 650 °C, under standard cathodic atmosphere (CO_2:O_2, 70:30).

Electrochemical measurements were carried out using a PGSTAT30, Autolab Ecochemie BV. The open circuit potential was registered as a function of time, interrupted when stable to perform impedance spectroscopy measurements. Electrochemical impedance spectroscopy has been carried out at the OCP value. The AC signal amplitude was of 5 mV, low enough to respect the system linearity. All the diagrams were recorded from 10^6 Hz to 1 mHz, using eight points per decade of frequency.

2.4. Solubility measurements

Small amounts of carbonates (about 0.4 g) were regularly withdrawn from the molten carbonate bulk during the electrochemical characterizations. Each sample was hand-milled and dissolved in HCl 3%, in the right proportion to get a 20 g L^{-1} carbonate concentration. It was then analyzed by ICP-AES, using a Liberty II Axial, Varian apparatus. Ni, Co and Fe have elements were determined. The calibration was performed for each separated element, from 10 ppm to 10 ppb, using Aldrich atomic absorption standard solutions, dissolved in 3% HCl, containing 20 g L^{-1} of the carbonates mixture, in order to work with the same matrix than the samples.

The raw results y_i consist in a weight concentration of element i (versus the A solution), converted in weight ratio x_i (taken into account the molten carbonate mixture) or molar ratio X_i using the following relations:

$$x_i = \frac{y_i}{A} \quad (A \text{ in g kg}^{-1})$$

$$X_i = x_i \frac{M_{\text{carbonate}}}{M_i}$$

2.5. SEM observations

Before and after exposure to the molten carbonate, under the MCFC cathode conditions, SEM observations coupled to EDS analysis were performed (HITACHI S2500). The surfaces and the inside of the pellets have been characterized. For the pellet inside, the samples have been broken and polished, using SiC papers (up to P1200). A thin layer of 30 nm of gold was deposited before SEM observations.

3. Results and discussion

3.1. Phase analysis

The prepared materials can be divided into three ternary subsystems. The compositional and phase details of the prepared materials are shown in Fig. 1. The phase details shown in this fig-

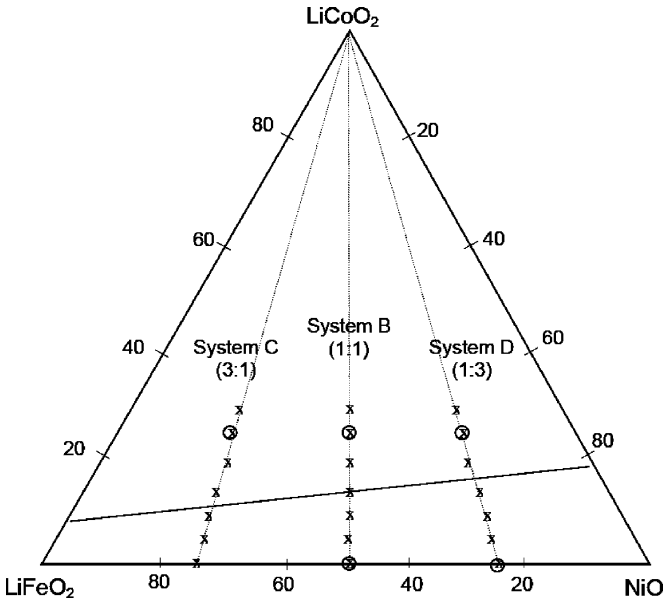

Fig. 1. The compositional and phase details of the prepared materials. The corresponding $LiFeO_2$:NiO molar ratios for the ternary sub-Systems B–D, are 1:1, 3:1 and 1:3 respectively. The proposed $LiFeO_2$–$LiCoO_2$–NiO solid solution boundary is marked in the figure. The material compositions used for electrochemical characterization and solubility studies are marked with circles.

ure are based on the XRD analysis performed on pellets sintered at 1000 °C for 2 h in static air. $LiFeO_2$–$LiCoO_2$–NiO ternary materials with constant molar ratios of $LiFeO_2$:NiO and varying $LiCoO_2$ contents between 0 and 25 mole% were prepared under these three ternary sub-systems. The corresponding $LiFeO_2$:NiO molar ratios for the sub-Systems B–D and are 1:1, 3:1 and 1:3, respectively.

According to XRD phase analysis, the ternary compositions containing low $LiCoO_2$ contents form $LiFeO_2$–$LiCoO_2$–NiO solid solutions of the *Fm*3*m* cubic rock-salt structure rich in $LiFeO_2$ and NiO. The apparent solid solution boundary is in between 10 and 15 mole% of $LiCoO_2$ for Systems B and C while it is slightly higher, in between 15 and 20 mole% of $LiCoO_2$, for System D.

3.2. DC electrical conductivity

The variation of the specific electrical conductivity of these ternary compositions with $LiCoO_2$ content, at 650 °C in cathode gas, is shown in Fig. 2. A similar trend of increasing conductivity with the content of $LiCoO_2$ in the material can be noticed in all these ternary compositions. The increase in $LiCoO_2$ content of the material increases the conductivity to a maximum, followed by a decrease in conductivity with further increasing of $LiCoO_2$ content. This conductivity maximum is slightly shifting towards the materials with higher $LiCoO_2$ content, with decreasing the $LiFeO_2$:NiO ratio in the system. The maximum is shifting from about 20 to 25 mole% of $LiCoO_2$ content, when the $LiFeO_2$:NiO ratio is changing from 3:1 (System C) to 1:3 (System D).

As shown in Fig. 2, when comparing the electrical conductivity among these ternary materials with the same $LiCoO_2$ content, the materials in System D (with the lowest $LiFeO_2$:NiO molar

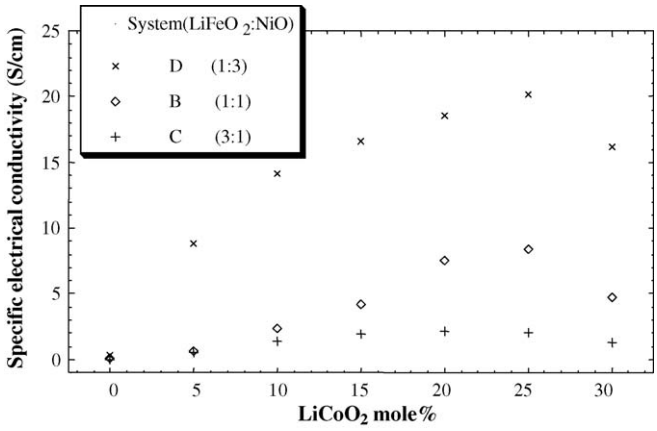

Fig. 2. The variation of the specific electrical conductivity of ternary compositions with $LiCoO_2$ content, at 650 °C in cathode gas (30% CO_2 + 70% air).

ratio, 1:3) show the highest conductivity. The materials in System C (with the highest $LiFeO_2$:NiO molar ratio, 3:1) show the lowest conductivity, while the conductivity of materials in System B lies in between. This behavior is identical to that of the $LiFeO_2$–NiO binary system [15]; the electrical conductivity decreases with increasing $LiFeO_2$ content in the material, due to the very low electrical conductivity of $LiFeO_2$.

Among the ternary materials, the materials which possess the highest electrical conductivity in the $LiFeO_2$–$LiCoO_2$–NiO ternary system, are multiphase materials. Considering mainly the electrical conductivity, the cathodes showing the highest effective conductivity in Systems B and D were selected for cell testing. The details of the electrochemical performance of these cell tested cathodes are found elsewhere [15,16]. In brief, the cell performance of the cathodes prepared from 20 and 25 mole% $LiCoO_2$ compositions of System D (D20 and D25, respectively) is much interesting and far better than other $LiFeO_2$–$LiCoO_2$–NiO cathodes prepared in this study. The cathodic *iR*-drop is far lower, while the polarization is in the same order with respect to those reported for $LiCoO_2$ cathodes [16]. It suggests the existence of a very low contact resistance between the cathode and the current collector compared to that of $LiCoO_2$ cathodes. Furthermore, the performance of these cathodes are almost comparable to that expected for the NiO cathode in a commercial fuel cell [19].

3.3. Solubility and electrochemical characterization studies

Dense pellets, sintered at 1000 °C for 2 h in air, were used for the solubility and electrochemical characterization studies. The geometrical surface area and the thickness of these pellets were about 0.8 cm^2 and 0.3 cm, respectively. The compositional details of the materials used for these studies are given in Table 1 (see also Fig. 1). For these studies, 0 mole% $LiCoO_2$ (binary compositions) of Systems B and D, and at 25 mole% $LiCoO_2$ (ternary compounds) of Systems B–D were used.

All these samples were previously analyzed and immersed in the melt for 200 h. Solubility determinations, given in Table 2, show that the nickel concentration is higher when $LiCoO_2$ is added to the binary compound. In effect, Ni concentration in

Table 1
Composition (in mole%) and reference of the studied samples

Name	NiO	$LiFeO_2$	$LiCoO_2$
B25	37.5	37.5	25
C25	18.75	56.25	25
D25	56.25	18.75	25
B0	50	50	0
D0	75	25	0

Table 2
Solubility measurements (wt ppm) after 200 h in Li–Na melt, at 650 °C, under cathode conditions

Name	Ni	Co	Fe
B25	3.0	0.80	Non relevant
C25	3.3	1.00	Non relevant
D25	1.5	0.40	Non relevant
B0	<0.6 ppm	–	<0.6 ppm
D0	<0.6 ppm	–	<0.6 ppm

the melt after immersion of B0 and D0 is lower than the detection limit of 0.6 wt ppm. In the case of the iron–nickel binary compound, the obtained values are not relevant and the dissolution can be neglected. The effect of the $LiCoO_2$ addition on the nickel solubility is relevant, but can be reduced by adjusting the ratio of NiO and $LiFeO_2$ in the ternary compound. From the series of three samples, where $LiCoO_2$ is fixed at 25%, D25 appears as the most interesting sample, presenting the lowest Ni and Co contents in the molten carbonate, after 200 h of immersion. Moreover, the EDS analysis of the pellet surface, realized before and after 200 h of immersion, clearly shows that the D25 compound is less affected than C25 and B25 compounds, as reported in Fig. 3. Only a slight variation of the Ni/Fe ratio can be noted.

Nevertheless, $LiCoO_2$ addition leads to an increase in the material conductivity, even under air as presented in Fig. 4. These measurements were carried out by impedance spectroscopy as a function of the temperature, and activation energies close to 0.45 and 0.6 eV were deduced from the respective slopes. This energy is quite high for pure electronic conductors, but was not measured under the cathode atmosphere. As proposed by

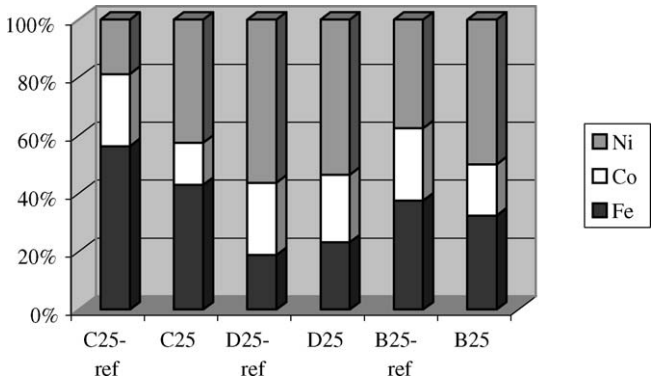

Fig. 3. Ni, Fe and Co composition of the pellet surface, before (ref) and after 200 h of immersion in Li–Na carbonate melt.

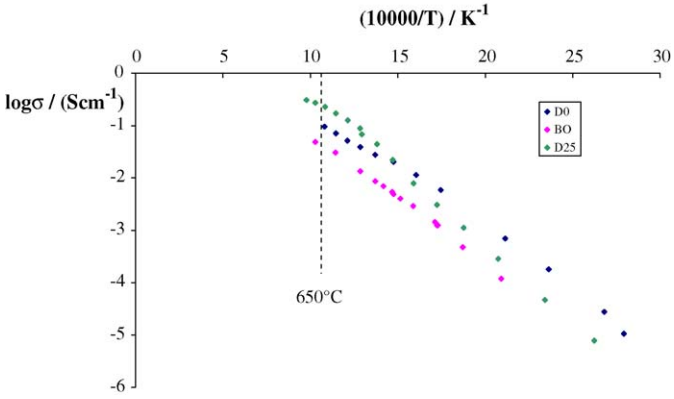

Fig. 4. Conductivity under air, as a function of the temperature in Arrhenius coordinates for B0, D0 and D25 samples.

Wijayasinghe et al. [15–17], $LiCoO_2$ and $LiFeO_2$ should be both proposed to compensate the electrical conductivity and the solubility of NiO, respectively.

In Fig. 5, are superimposed the impedance diagrams recorded after 150 h of immersion, for each compositions, i.e. D0, D25, B25 and C25 compounds. It clearly reveals that the resistance can be largely decreased, by adding $LiCoO_2$, (from 250 Ω for D0 to 20 Ω for D25, thus more than a factor of 10), and shows the positive effect of a lower $LiFeO_2$/Ni ratio. The evolution of the diagrams versus time is also a positive argument for selecting the D System compounds. As can be seen in Fig. 6a and b, for the B25 and C25 samples, the resistance continuously increased with the time while an opposite variation is globally observed for D25 (Fig. 6c).

Thus, due to the previous characterizations, the results are focused on the influence of the $LiCoO_2$ addition, for a composition based on a ratio of 1:3 of $LiFeO_2$:NiO. In terms of impedance spectroscopy characteristics, the high frequency contribution resistance decreased slightly during the immersion, as can be seen in Fig. 6c for D25 sample. The same behavior was observed for D0. Thus, the $LiCoO_2$ content does not seem to be responsible of this phenomenon. This could result from the

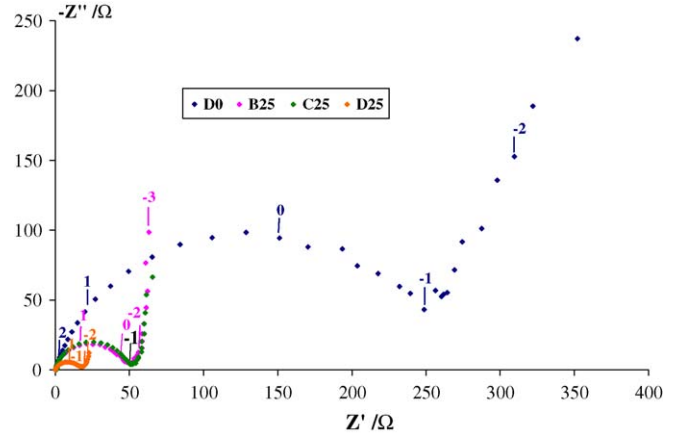

Fig. 5. Impedance diagrams recorded at the OCP values, for the D0, D25, B25 and C25 samples, after 155 h of immersion. The frequencies logarithms are reported in the figure.

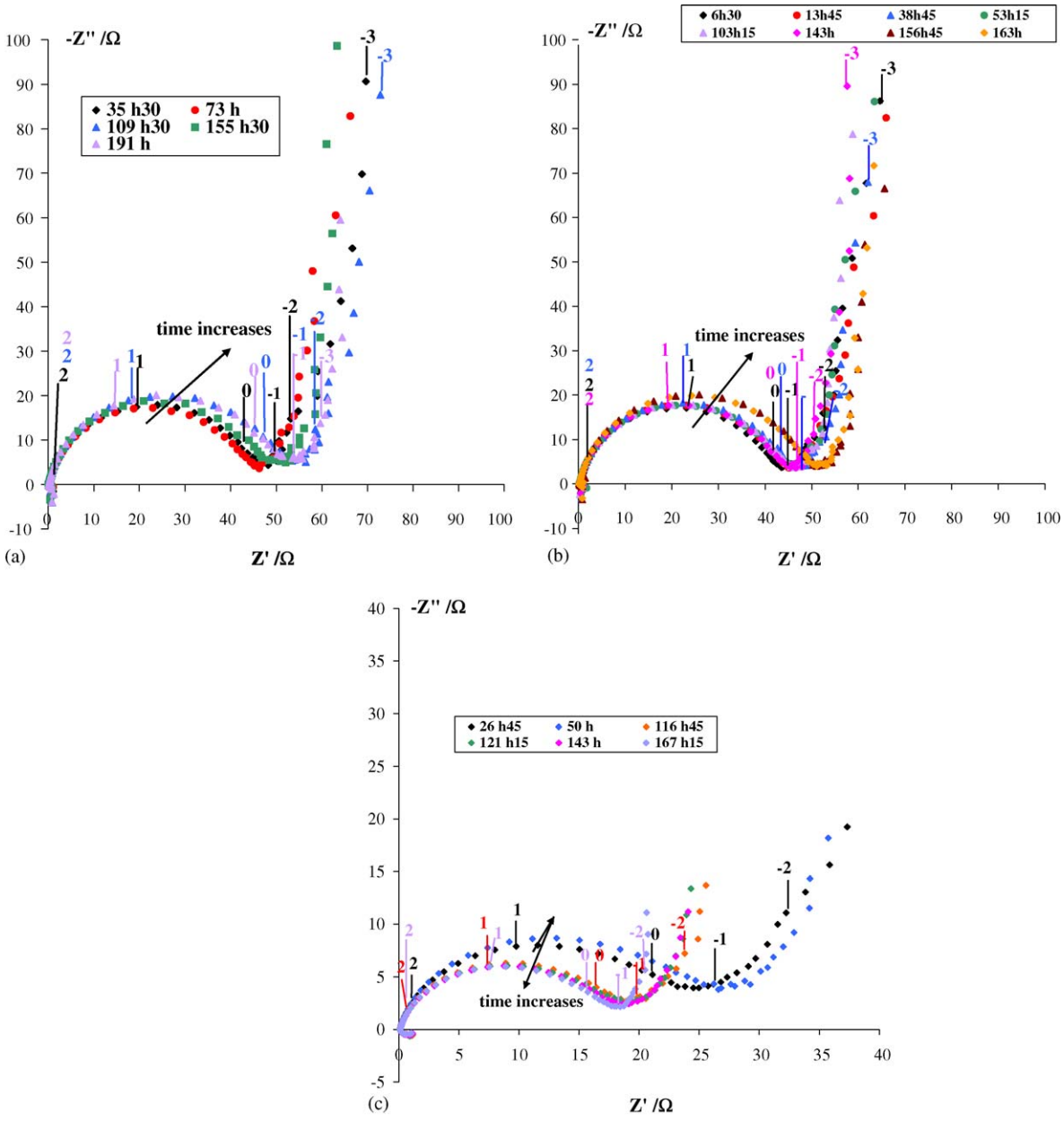

Fig. 6. Impedance diagrams at different times, up to 190 h of immersion: (a) B25 compound; (b) C25 compound; (c) D25 compound.

crystallinity increase observed by SEM, comparing the surface morphology before and after the immersion. As can be seen in Fig. 7a, the porosity of the D0 pellet is an open porosity, the grain size is lower than 1 μm and the shape not clearly defined. After 200 h of immersion in the Li–Na electrolyte, under MCFC standard cathode conditions, the porosity is still present and is kept open, but a grain growth can be noted. Grain size is about 2–3 μm (Fig. 7b).

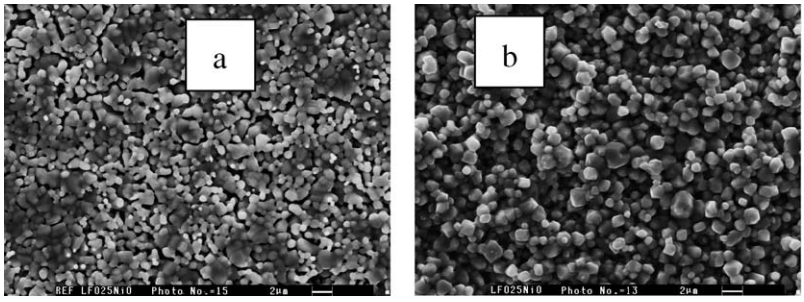

Fig. 7. Microstructure of the surface of D0 pellet, before immersion into the melt (a) and after 200 h (b).

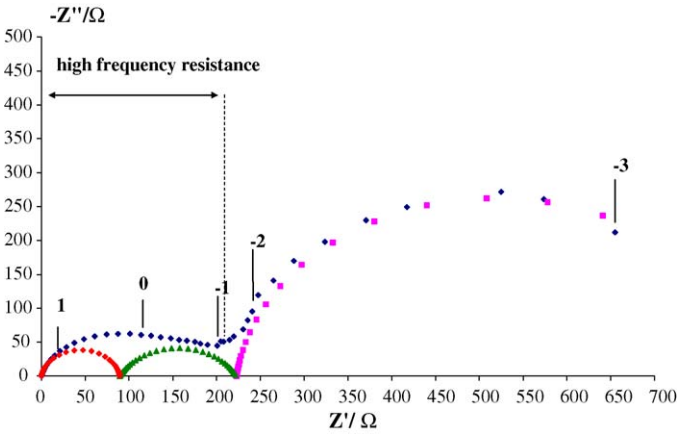

Fig. 8. Typical impedance diagram recorded for D0 sample (close symbol). An example of the diagram decomposition is superimposed (open symbol). The logarithm of the measurement frequency is reported on the diagram.

Comparing the impedance diagrams in Figs. 8 and 9, in both cases two main parts can be distinguished. Up to 100 mHz, the so-called high frequency part, composed of two semi-circles, more defined for D0 than for D25. For the lowest frequencies, the shape of the impedance diagram depends on the composition and an evolution can be noted during the immersion in the molten carbonate mixture. A large semi-circle is observed for the binary compound. It is more linear for D25 and the slope tends to increase with the time. Unfortunately, it is still quite difficult to explain this behavior. However, a modification of the electrolyte/cathode interface can be suggested, leading to a more blocking effect when $LiCoO_2$ is added.

The most significant fact consists in the difference between the high frequency part resistance, with a factor 10 from D0 to

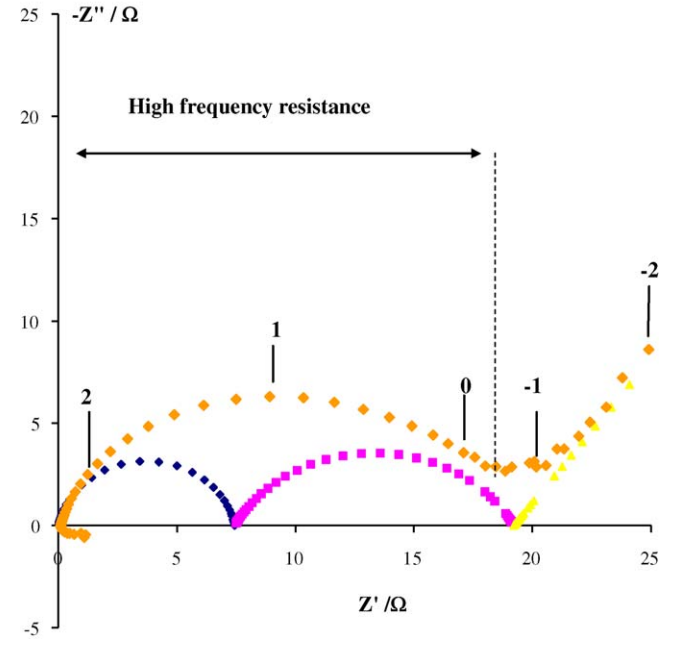

Fig. 9. Typical impedance diagram recorded for D25 sample (close symbol). An example of the diagram decomposition is superimposed (open symbol). The logarithm of the measurement frequency is reported on the diagram.

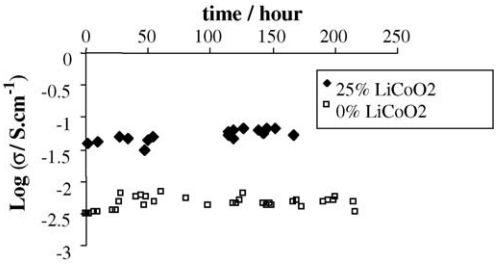

Fig. 10. Variation of the high frequency contribution conductivity vs. time for the D0 and D25 pellets.

D25: close to 200 and 20 Ω, respectively. These variations are represented in terms of conductivity in Fig. 10, avoiding taking into account the geometrical factors, as a function of the time for both compositions. This high frequency part could be attributed to the charge transfer phenomenon, according to Pérez et al. [20] and Huang et al. [21], and thus the presence of $LiCoO_2$ would accelerate it. Pérez et al. have also discussed the presence of one arc or two semi-arcs in the high frequency part, showing that it was depending on the species involved in the limiting processes. The discussion of the mechanisms is still going on for the ternary compounds presented in this study, and does not constitute the main purpose of this paper. It should be added that this high frequency resistance tends to decrease with the immersion time, but the variations are not so important, mainly for the ternary D25 compound.

According to all the results obtained from this study the composition of 15–30 mole% $LiCoO_2$ in System D shows sufficient electrical conductivity for an MCFC cathode. Also fuel cell testing has revealed very promising results for 20 and 25 mole%, respectively in System D [16]. The considerably lower solubility of D25, when compared to the state-of-the-art NiO, is surely a big advantage for MCFC cathode application.

4. Conclusion

This study reveals the ability of improving electrical conductivity, adequate for MCFC cathode application, by controlling the $LiCoO_2$ content in ternary compositions. The ternary compositions containing low $LiCoO_2$ contents form $LiFeO_2$–$LiCoO_2$–NiO solid solutions of the *Fm*3*m* cubic rock-salt structure rich in $LiFeO_2$ and NiO. The apparent solid solution boundary is in between 10 and 15 mole% of $LiCoO_2$ for Systems B ($LiFeO_2$:NiO = 1:1) and C ($LiFeO_2$:NiO = 3:1), while it is slightly high, in between 15 and 20 mole% of $LiCoO_2$, for System D ($LiFeO_2$:NiO = 1:3).

$LiCoO_2$ addition to a binary compound of the system NiO–$LiFeO_2$ was studied considering different aspects. While $LiFeO_2$ permits a decrease in the Ni dissolution, it can also affect the cobalt solubility. $LiCoO_2$ permits to get better electrical and electrochemical performances for such compounds. The high frequency impedance contribution is not depending on the cobalt content: two semi-circles composed this part of the diagram, in the same frequency range (from 1 MHz to 100 mHz). Nevertheless, the corresponding resistance is largely decreased, by a factor 10, when 25% of $LiCoO_2$ is added to the binary initial

composition. Thus, the charge transfer process will be accelerated with a cathode material containing the three elements, in an optimized ratio.

Taking into account solubility, electrical conductivity, as well as electrochemical performance in the fuel cell, the compositions with 20–25 mole% of $LiCoO_2$ in System D can be proposed as viable alternative MCFC cathode materials.

References

[1] J.R. Selman, in: L.J.M.J. Blomen, M.N. Mugerwa (Eds.), Fuel Cell Systems, Plenum Press, New York, 1993, pp. 345–463.
[2] K. Tanimoto, M. Yanagida, T. Kojima, Y. Tamiya, H. Matsumoto, Y. Miyazaki, J. Power Sources 72 (1998) 77–82.
[3] M. Cassir, C. Belhomme, Plasmas Ions 1 (1999) 3–15.
[4] H. Morita, M. Komoda, Y. Mugikura, Y. Izaki, T. Watanabe, Y. Masuda, T. Matsuyama, J. Power Sources 112 (2002) 509–518.
[5] K. Tanimoto, T. Kojima, M. Yanagida, K. Nomura, Y. Miyazaki, J. Power Sources 131 (2003) 256–260.
[6] M.J. Escudero, T. Rodrigo, L. Mendoza, M. Cassir, L. Daza, J. Power Sources 140 (2005) 81–87.
[7] L. Mendoza, A. Ringuedé, M. Cassir, A. Galtayries, J. Electroanal. Chem. 576 (2005) 147–160.
[8] L. Giorgi, M. Carewska, M. Patriarca, S. Scaccia, E. Simonetti, A.D. Bartolomeo, J. Power Sources 49 (1994) 227–243.
[9] J.L. Smith, G.H. Kucera, A. Brown, in: J.R. Selman, D.A. Shores, H.C. Maru, I. Uchida (Eds.), Proceedings of Second Symposium on Molten Carbonate Fuel Technology, The Electrochemical Society Proceeding Series, Pennington, NJ, 1990, pp. 226–246 (PV 90–16).
[10] C. Lagergren, A. Lundblad, B. Bergman, J. Electrochem. Soc. 141 (1994) 2959–2966.
[11] A. Lundblad, S. Schwartz, B. Bergman, J. Power Sources 90 (2000) 224–230.
[12] R.C. Makkus, K. Hemmes, J.H.W. de Wit, J. Electrochem. Soc. 141 (1994) 3429–3438.
[13] I. Bloom, M.T. Lanagan, M. Krumpelt, J.L. Smith, J. Electrochem. Soc. 146 (1999) 1336–1340.
[14] T. Kudo, K. Kihara, Y. Hisamitsu, Q. Yu, M. Mohamedi, I. Uchida, J. Mater. Chem. 12 (2002) 2496–2500.
[15] A. Wijayasinghe, B. Bergman, C. Lagergren, J. Electrochem. Soc. 150 (5) (2003) A558–A564.
[16] A. Wijayasinghe, C. Lagergren, B. Bergman, Fuel Cells 2 (3) (2002) 181–188.
[17] A. Wijayasinghe, B. Bergman, C. Lagergren, Electrochim. Acta 49 (2004) 4709–4717.
[18] Pechini, M.P., U.S Patent no. 3,330,697, (1967).
[19] C. Yuh, R. Johnsen, M. Farooque, H. Maru, J. Power Sources 56 (1995) 1–10.
[20] F.J. Pérez, D. Duday, M.P. Hierro, C. Gomez, M. Romero, M.T. Casais, J.A. Alonso, Martinez, L. Daza, J. Power Sources 86 (2000) 309–315.
[21] B. Huang, F. Li, Q. Yu, G. Chen, B.Y. Zhao, K.A. Hu, J. Power Sources 128 (2004) 135–144.